J Neurogastroenterol Motil, Vol. 28 No. 4 October, 2022
pISSN: 2093-0879 eISSN: 2093-0887
https://doi.org/10.5056/jnm21183
Journal of Neurogastroenterology and Motility

Original Article

Relationship Between Intestinal Slow-waves, Spike-bursts, and Motility, as Defined Through High-resolution Electrical and Video Mapping

Sachira Kuruppu,[1] Leo K Cheng,[1,2,3] Recep Avci,[1] Timothy R Angeli-Gordon,[1] and Nira Paskaranandavadivel[1]*

[1]Auckland Bioengineering Institute, University of Auckland, New Zealand; [2]Riddet Institute, Center of Research Excellence, New Zealand; and [3]Department of Surgery, Vanderbilt University, Nashville, USA

Background/Aims
High-resolution extracellular mapping has improved our understanding of bioelectric slow-wave and spike-burst activity in the small intestine. The spatiotemporal correlation of electrophysiology and motility patterns is of critical interest to intestinal function but remains incompletely defined.

Methods
Intestinal jejunum segments from in vivo pigs and rabbits were exteriorized, and simultaneous high-resolution extracellular recordings and video recordings were performed. Contractions were quantified with strain fields, and the frequencies and velocities of motility patterns were calculated. The amplitudes, frequencies, and velocities of slow-wave propagation patterns and spike-bursts were quantified and visualized. In addition, the duration, size and energy of spike-burst patches were quantified.

Results
Slow-wave associated spike-bursts activated periodically at 10.8 ± 4.0 cycles per minute (cpm) in pigs and 10.2 ± 3.2 cpm in rabbits, while independent spike-bursts activated at a frequency of 3.2 ± 1.8 cpm. Independent spike-bursts had higher amplitude and longer duration than slow-wave associated spike-bursts (1.4 ± 0.8 mV vs 0.1 ± 0.1 mV, $P < 0.001$; 1.8 ± 1.4 seconds vs 0.8 ± 0.3 seconds, $P < 0.001$ in pigs). Spike-bursts that activated as longitudinal or circumferential patches were associated with contractions in the respective directions. Spontaneous peristaltic contractions were elicited by independent spike-bursts and travelled slower than slow-wave velocity (3.7 ± 0.5 mm/sec vs 10.1 ± 4.7 mm/sec, $P = 0.007$). Cyclic peristaltic contractions were driven by slow-wave associated spike-bursts and were coupled to slow-wave velocity and frequency in rabbit (14.2 ± 2.3 mm/sec vs 11.5 ± 4.6 mm/sec, $P = 0.162$; 11.0 ± 0.6 cpm vs 10.8 ± 0.6 cpm, $P = 0.970$).

Conclusions
Motility patterns were dictated by patterns of spike-burst patches. When spike-bursts were coupled to slow-waves, periodic motility patterns were observed, while when spike-bursts were not coupled to slow-waves, spontaneous aperiodic motility patterns were captured.

(J Neurogastroenterol Motil 2022;28:664-677)

Key Words
Electrophysiology; Intestinal motility; Peristalsis; Video recording; Swine

Received: September 10, 2021 Revised: December 1, 2021 Accepted: December 17, 2021

*Correspondence: Nira Paskaranandavadivel, PhD
Auckland Bioengineering Institute, University of Auckland, Private Bag 92019, Auckland 1142, New Zealand
Tel: +64-9-923-3175, Fax: +64-9-367-7157, E-mail: nira.pask@auckland.ac.nz

Introduction

The intestinal musculature consists of longitudinal and circular muscle layers, whose coordinated contraction and relaxation facilitates breakdown and digestion of food via motility.[1] Intestinal motility is governed by a multitude of regulatory mechanisms including neuronal, hormonal and myogenic means.[2-4] The enteric nervous system, also known as the "gut brain," mediates motility through motor neurons present between the 2 muscle layers.[3] These motor neurons release neurotransmitters to activate selective ion channels in smooth muscle cells that directly or indirectly facilitate calcium entry to initiate muscle contraction.[5] Myogenic mediation of motility is facilitated through interstitial cells of Cajal (ICC), the pacemaker cells of the gastrointestinal tract. The ICC network generates waves of depolarization called slow-waves, which periodically increases the probability of voltage-dependent calcium channels to open.[6] When the slow-waves exceed a threshold voltage, inward calcium currents are activated in smooth muscle cells, leading to contraction.[7]

The coordinated activations of myogenic and neural regulatory mechanisms lead to varying motility patterns that accomplish different roles. Non-propagating circumferential contractions, known as segmental contractions, are the most common type of contractions in the intestine.[8] They help break down intraluminal content, and rhythmic segmental contractions, known as the segmentation motility pattern, help with both mixing and breaking down.[9] Propagating circumferential contractions, also known as peristaltic contractions, transport intraluminal content along the intestine.[10-12] Longitudinal contractions, also known as pendular contractions, help with mixing.[13] Some of these motility patterns, such as spontaneous peristalsis in the guinea-pig colon and in W/W^v knockout mouse intestine (mice possessing a mutated kit gene that impairs ICC growth), are mediated via neural pathways.[10,14] In contrast, cyclic peristaltic contractions, such as ripple contractions in the colon, are myogenically mediated.[14] Other cyclic peristaltic contractions defined as propagating oscillations and peristalsis in mouse intestine,[10,15] are driven by the coordination of both neurogenic and myogenic mechanisms.

Extracellular serosal electrical recordings reveal 2 types of bioelectrical events that govern motility: (1) slow-waves generated and propagated by ICC appear as an omnipresent rhythmic change in potential, and (2) fast fluctuations called spike-bursts[16] which are believed to be the inward calcium currents in the smooth muscle cells.[17-19] Spike-bursts are directly associated with contractions, and have been observed to increase intraluminal pressure and outflow.[20,21] Spike-bursts can be neurogenic, which are eliminated by neural inhibitory agents, or myogenic, which are resistant to neural inhibitory agents.[22]

Even though all spike-bursts induce contractions, there is evidence to suggest that their activation patterns dictate the type of contraction. Peristaltic contractions have been reported to be driven by spike-bursts propagating along the length of the intestine as a sheath.[23] Two types of peristaltic contractions have been reported. Peristaltic contractions driven by spike-bursts that cause outflow in synchrony with slow-waves have been observed in healthy animal models,[10,15] and peristaltic contractions driven solely by spike-bursts independent of slow-waves have been observed in both healthy animal models and W/W^v knockout mice that lack ICC.[10,23] Longitudinal activation of spike-bursts associated with slow-waves have been observed with pendular contractions.[24] Although the above studies indicate that spike-burst activation pattern and their affinity to slow-waves play a key role in determining the motility pattern, they do not show a clear spatiotemporal correlation between the spike-burst activation patterns and the motility patterns due to technological limitations. Some studies have predominantly focused on the bioelectrical activity and have not mapped or quantified the motility patterns.[10,23] Other studies have utilized 1-dimensional electrode arrays and motility measurements, therefore, have not clearly captured or correlated the 2-dimensional spike-burst, slow-wave activations on the tissue surface with the surface deformations. In addition, existing studies have predominantly been performed in tissue baths,[10,15,23,24] and may not represent the integrative electrophysiological state of the gut.

High-resolution (HR) electrode arrays can define the spatial activations of slow-waves and spike-bursts by simultaneously recording from a 2-dimensional area of the intestinal surface.[25-29] New video mapping techniques have recently been developed to quantify surface strain fields during contractions in the in vivo intestine.[30] Integrating these methods provides the opportunity to study the dynamics between slow-waves, spike-bursts, and motility in comprehensive spatial detail. The aim of this study is to apply these new HR electrical and video mapping techniques to identify how spatiotemporal activation of slow-waves and spike-bursts are related to differing motility patterns in the in vivo small intestine.

Materials and Methods

Experimental Setup

Experiments were performed under the ethical approval of the

University of Auckland Animal Ethics Committee (Approval No. 001811, 002124 and AEC3090). Experiments were performed in vivo on female cross-breed, weaner pigs, and female New Zealand white rabbits, both established models of small intestine slow-wave and spike-burst investigation using HR mapping methods.[27,31] The use of both animal species in this study allowed for a broad investigation to account for potential inter-species variability. Animal care, preparation and anesthesia were performed as previously described.[27,31] The experimental arrangement is shown in Figure 1. In summary, a midline laparotomy was performed, and a section of the jejunum was exteriorized and placed on top of an electrode array that consisted of 128 channels arranged in a 16 × 8 grid with 4 mm inter-electrode spacing. Electrical activity was acquired using a passive, unipolar ActiveTwo system (BioSemi, Amsterdam, Netherlands) at a sampling frequency of 512 Hz. The jejunum section was distended by injecting warm saline (10-15 mL) into the lumen with a 20 g needle, to induce contractions.[10,15]

Mechanical contractions of the intestine were simultaneously captured using a validated cross-polarized camera setup, as previously described.[30] In brief, the contractions were recorded at 20 frames per second, with a Blackfly S machine vision camera (BFS-U3-50S5M-C; Teledyne FLIR, Wilsonville, Oregon, USA), positioned as shown in Figure 1. The camera and the light source were perpendicularly polarized to eliminate specular reflection. The video frames (2448 × 2048 pixels) were synchronized to the electrical activity by recording a transistor-transistor logic pulse generated by the camera during frame capture to the BioSemi ActiveTwo system.

Bioelectrical Signal Processing

Bioelectrical data analysis was performed using the Gastrointestinal Electrical Mapping Suite GEMS.[32] The baseline drift of the electrical signals was identified by first applying a median filter (window size 1.5 seconds) and then a Savitzky-Golay filter (window size 1.5 seconds, polynomial order 2) to the raw signals, which was then deducted to remove the baseline drift. The baseline corrected signals were then filtered to remove high frequency noise by first deducting the median of all the signals and then applying a Savitzky-Golay filter (window size 0.1 seconds, polynomial order 9). Slow-wave events were manually marked and grouped into propagating events. The slow-wave cycles were plotted as spatiotemporal isochronal maps, defined here as activation time maps, to visualize the slow-wave propagation patterns.[33]

Frequency and velocity metrics were computed from marked slow-wave events. The slow-wave period was computed as the time difference between adjacent slow-wave events in each electrode. The frequency was computed as the mean reciprocal of slow-wave period across all electrodes and reported in cycles per minute (cpm). The velocity of slow-waves was computed using a finite difference approach with Gaussian smoothing to reduce artifacts.[34]

Spike-burst events were identified and grouped using an automated method previously described.[29] In brief, slow-waves were removed by performing suppression of artifacts by local polynomial approximation[35,36] on the baseline corrected signals (window size 300 milliseconds). The start and end times of spike-bursts were identified by computing the fourth order differential

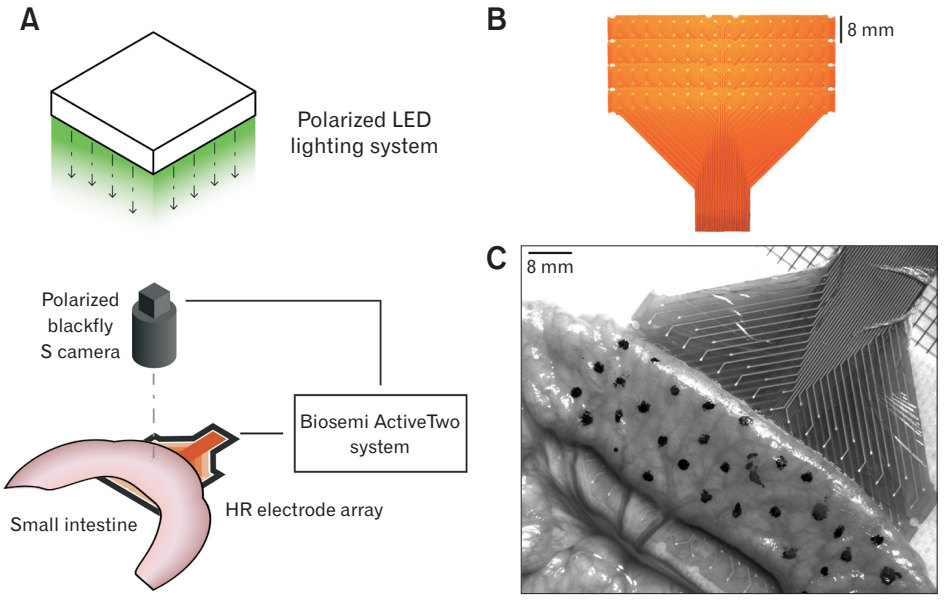

Figure 1. Simultaneous bioelectrical and video mapping method. (A) Arrangement of the cross-polarized camera setup and the electrode array on the intestine. Camera exposure is recorded along with the bioelectrical signals by the BioSemi ActiveTwo system for synchronization. (B) Flexible electrode array used for high-resolution (HR) bioelectrical mapping (16 × 8 configuration; 4 mm spacing). (C) Intestine as visible from the camera, placed over the flexible electrode array. LED, light emitting diode.

energy operator transform of the resulting signals, after which an empirical threshold (20 × approximate standard deviation of the energy transforms) was applied. The detected spike-burst events were clustered using a region growing method to identify spatial regions known as spike-burst patches.[37] Spike-bursts that activated in a periodic manner with the slow-wave cycles in the signal traces were identified as slow-wave associated spike-bursts, and those that activated independently in an aperiodic manner were identified as independent spike-bursts.

Amplitude and duration of spike-bursts and spike-burst patches were calculated. The duration of a spike-burst was taken as the difference between its start and end time. The amplitude of a spike-burst was taken as the difference between the maximum and minimum voltage levels during the spike-burst. The amplitude and duration of a spike-burst patch were defined as the mean amplitude and duration of all its spike-bursts, respectively. The size of a spike-burst patch was computed as the area of the electrode array activated by its spike-bursts (mm^2), and the energy of spike-burst patches was defined as the product of their amplitude, duration and patch size ($\mu V \cdot sec \cdot mm^2$). In addition, the frequency of slow-wave associated spike-bursts was calculated using the spike-burst start times, using the same algorithm for slow-wave frequency calculation. The velocities of propagating spike-burst patches were computed using the start times of their spike-bursts, via the same algorithm for slow-wave velocity estimation.

Slow-wave and spike-burst interactions with motility patterns were visualized by overlaying these events onto the video recordings of the intestine. The pixel locations of each electrode of the array were identified, and their slow-wave/spike-burst activations were spatially interpolated onto the video frames. These videos were used to analyze the spatiotemporal relationships between slow-waves, spike-bursts, and motility.

Quantification of Contractions

Contractions were quantified using a validated free-form deformation based method.[30] The geometry of the intestine was modeled using a biquadratic B-spline mesh, and the contractions were quantified by computing Green-Lagrange strain based on the change in the geometry. Motility patterns were presented as spatiotemporal maps of transverse strain for circumferential contractions, and longitudinal strain for longitudinal contractions, along the length of the intestine. Segmental and pendular contractions appeared as horizontal bands of negative strain in the transverse and longitudinal strain maps, respectively. Peristaltic contractions appeared as diagonal bands of negative strain. The strength of the contractions was defined as the mean strain, and the velocity of propagating contractions was calculated as the gradient of the diagonal bands. The frequency of periodic contractions was calculated as the mean reciprocal of the period between the contractile events. The magnitude, velocity, and frequency of contractions were quantitatively compared with slow-waves and spike-bursts.

Statistical Methods

All values are reported as mean ± standard deviation. Wilcoxon rank sum test was used as the statistical test to identify significant differences in the electrical parameters (amplitudes and durations) of slow-wave associated and independent spike-bursts. Pearson correlation was used to identify the trends between the level of contraction and the spike-burst patch amplitude, duration, size, energy. $P < 0.05$ was considered significant.

Table. Motility Patterns and the Relationship Between Spike-bursts and Slow-waves Observed During Experiments

Experiment	Baseline		Distended	
	Motility patterns	Spike-burst type	Motility patterns	Spike-burst type
Pig 1	Segmental, pendular	ISB, SWASB	N/A	N/A
Pig 2	—	—	Segmental, Spontaneous peristalsis	ISB
Pig 3	Pendular	SWASB	Segmental	ISB
Pig 4	—	—	Segmental, Spontaneous peristalsis	ISB
Pig 5	—	—	Segmental	ISB
Pig 6	—	—	Segmental	ISB
Rabbit 1	Cyclic peristalsis	SWASB	Cyclic peristalsis	SWASB
Rabbit 2	Pendular	SWASB	—	SWASB
Rabbit 3	Pendular	SWASB	N/A	N/A

Spike-bursts either occurred with slow-wave cycles (slow-wave associated spike-bursts [SWASB]) or independently to slow-waves (independent spike-bursts [ISB]). Not applicable (N/A) indicates not performed and dash indicates no activity.

Results

Experiments were performed in pigs (n = 6, 41.7 ± 2.5 kg) and rabbits (n = 3, 4.0 ± 0.7 kg), with a mean duration of 5 ± 4 minutes in baseline and 4 ± 2 minutes in distended recordings. Slow-waves in the jejunum occurred at 12.6 ± 2.3 cpm in the pig studies and 10.8 ± 1.5 cpm in the rabbit studies. Both slow-wave associated spike-bursts and independent spike-bursts were observed in baseline and distended experiments as shown in Table.

Spike-bursts occurred in conjunction with contractions. Slow-wave associated spike-bursts occurred with slow-wave cycles at 10.8 ± 4.0 cpm in pigs (slow-wave frequency for this subset was 11.8 ± 0.8 cpm), 10.2 ± 3.2 cpm in rabbits (slow-wave frequency for this subset was 10.8 ± 1.4 cpm), and could be distinctly identified from aperiodic independent spike-bursts that occurred less frequently (3.2 ± 1.8 cpm spike-burst frequency vs 12.0 ± 2.0 cpm slow-wave frequency for this subset in pigs). Rabbits did not exhibit independent spike-bursts. The independent spike-bursts and slow-wave associated spike-bursts displayed different electrical characteristics as shown in Figure 2. Independent spike-bursts observed with segmental and spontaneous peristaltic contractions had a larger morphology than the slow-wave associated spike-bursts observed with cyclic peristalsis and pendular contractions. The independent spike-bursts had a higher mean amplitude (1.4 ± 0.8 mV vs 0.1 ± 0.1 mV, $P < 0.001$ in pigs; 0.1 ± 0.1 mV slow-wave associated spike-bursts in rabbits; Fig. 2B) and a higher mean duration (1.8 ± 1.4 seconds vs 0.8 ± 0.3 seconds, $P < 0.001$ in pigs; 0.4 ± 0.2 seconds slow-wave associated spike-bursts in rabbits; Fig. 2D).

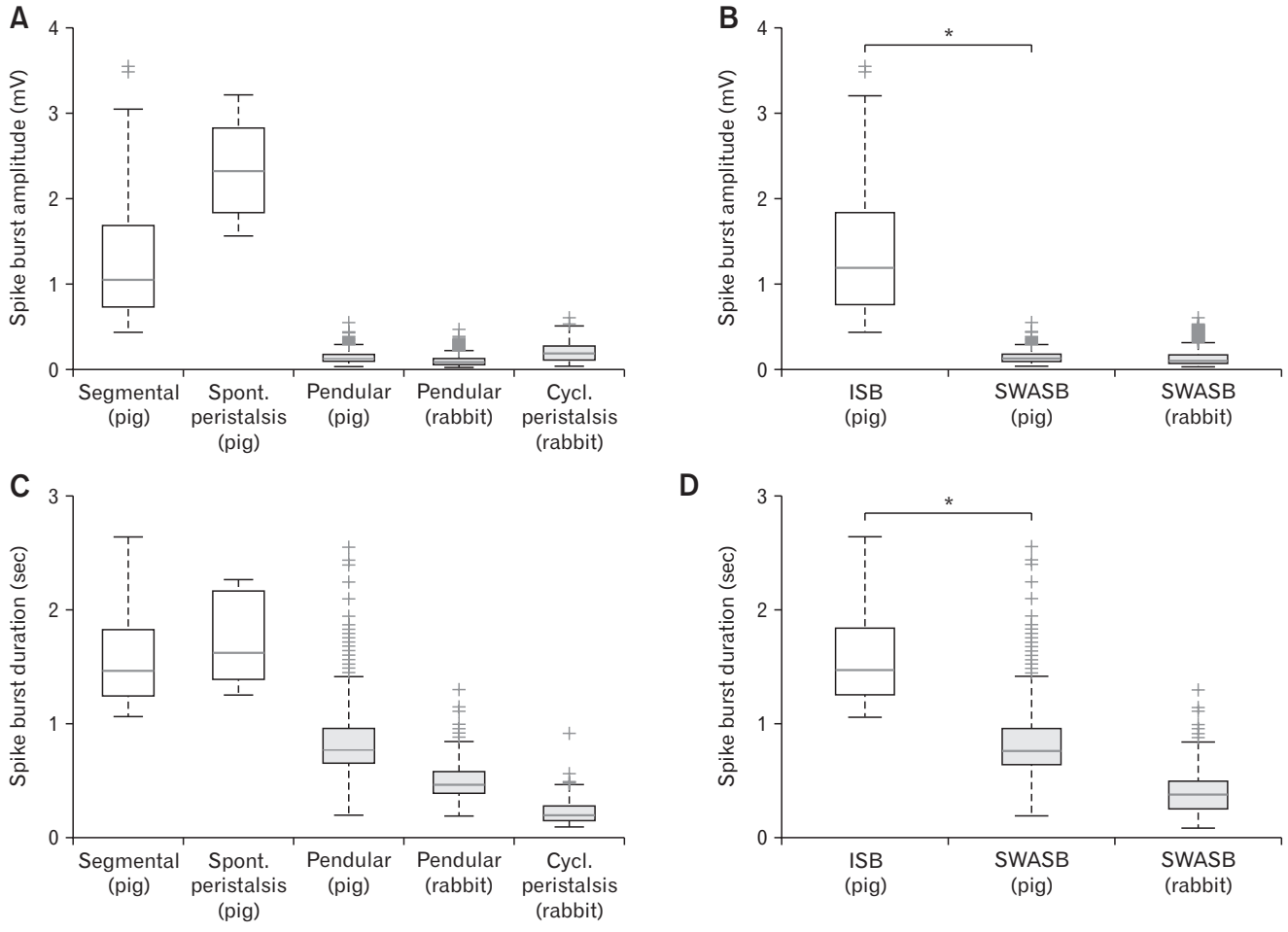

Figure 2. Electrical parameters of independent spike-bursts (ISB, white box plots) and slow-wave associated spike-bursts (SWASB, grey box plots). (A) Amplitudes of spike-bursts observed during motility patterns in each species. (B) Amplitudes of ISBs and SWASBs in each species. ISBs had significantly higher amplitude than SWASBs (*$P < 0.001$ within pigs). (C) Durations of spike-bursts observed during motility patterns in each species. (D) ISBs had significantly higher duration than SWASBs (*$P < 0.001$ within pigs). Spont., spontaneous; Cycl., cyclic.

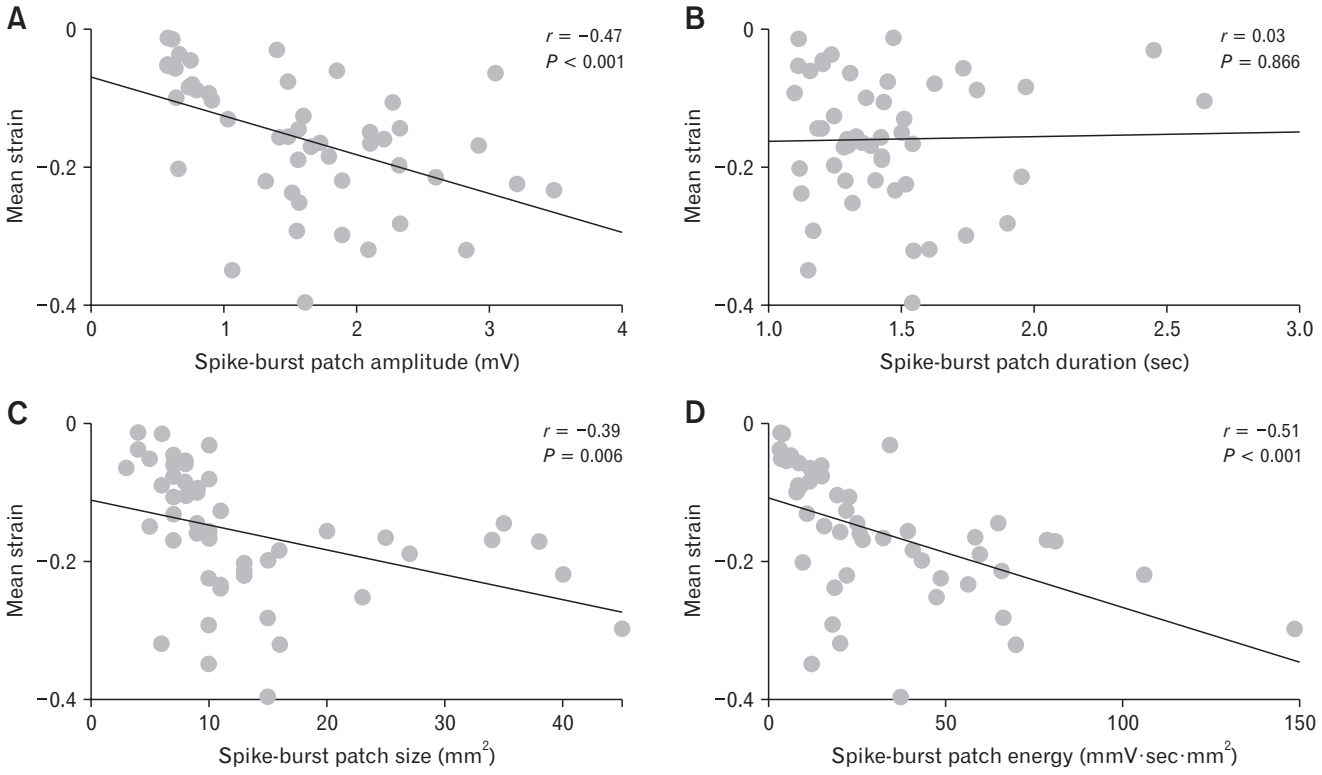

Figure 3. Correlation between spike-burst patch parameters and the level of contraction associated with them quantified by mean strain. (A) Spike-burst patch amplitude showed significant correlation with the level of contraction. (B) Spike-burst duration did not show a correlation with the level of contraction. (C) Spike-burst patch size, and (D) spike-burst patch energy displayed significant correlations with the level of contraction.

Spatially, spike-bursts activated as circumferential and longitudinal patches, and displayed a one-to-one relationship with intestinal contractions. The relationship between their electrical parameters and the level of deformations was analyzed using 48 segmental contractions as shown in Figure 3. There were significant correlations between the level of contraction indicated by negative strain and the amplitude ($r = -0.47$, $P < 0.001$; Fig. 3A), patch size ($r = -0.39$, $P = 0.006$; Fig. 3C), and the energy ($r = -0.51$, $P < 0.001$; Fig. 3D) of the spike-burst patches.

Segmental Contractions

Segmental contractions (n = 64) were observed in pigs. These contractions were driven by independent spike-bursts with a mean amplitude of 1.3 ± 0.7 mV and a mean duration of 1.8 ± 1.5 seconds. A representative example of the underlying bioelectrical activity during segmental contractions is shown in Figure 4. These non-propagating circular contractions caused the intestine to contract by 16 ± 9% and registered as horizontal bands of negative strain in the transverse strain maps (Fig. 4A). During segmental contractions spike-bursts activated as circumferential spike-burst patches as shown in Figure 4B. The spike-bursts were not coupled to the slow-waves as seen in the slow-wave activation map in Figure 4C, and the electrical traces in Figure 4D.

The spatiotemporal correlation of circumferential spike-burst patches with segmental contractions and their lack of correlation to slow-waves are more clearly shown in Supplementary Video 1.

Spontaneous Peristaltic Contractions

Spontaneous peristaltic contractions (n = 11) were also observed in pigs. These contractions were driven by independent spike-bursts with a mean amplitude of 2.3 ± 0.6 mV and a mean duration of 1.8 ± 0.8 seconds. A representative example of the underlying bioelectrical activity during spontaneous peristalsis is shown in Figure 5. These longitudinally propagating circumferential contractions caused the intestine to circumferentially contract by 36 ± 4% and registered as diagonal bands of negative strain in the transverse strain maps (Fig. 5A). During spontaneous peristaltic contractions spike-bursts activated as longitudinally propagating circumferential spike-burst patches as shown in Figure 5B. In other words, spike-bursts rapidly propagating around the circumference

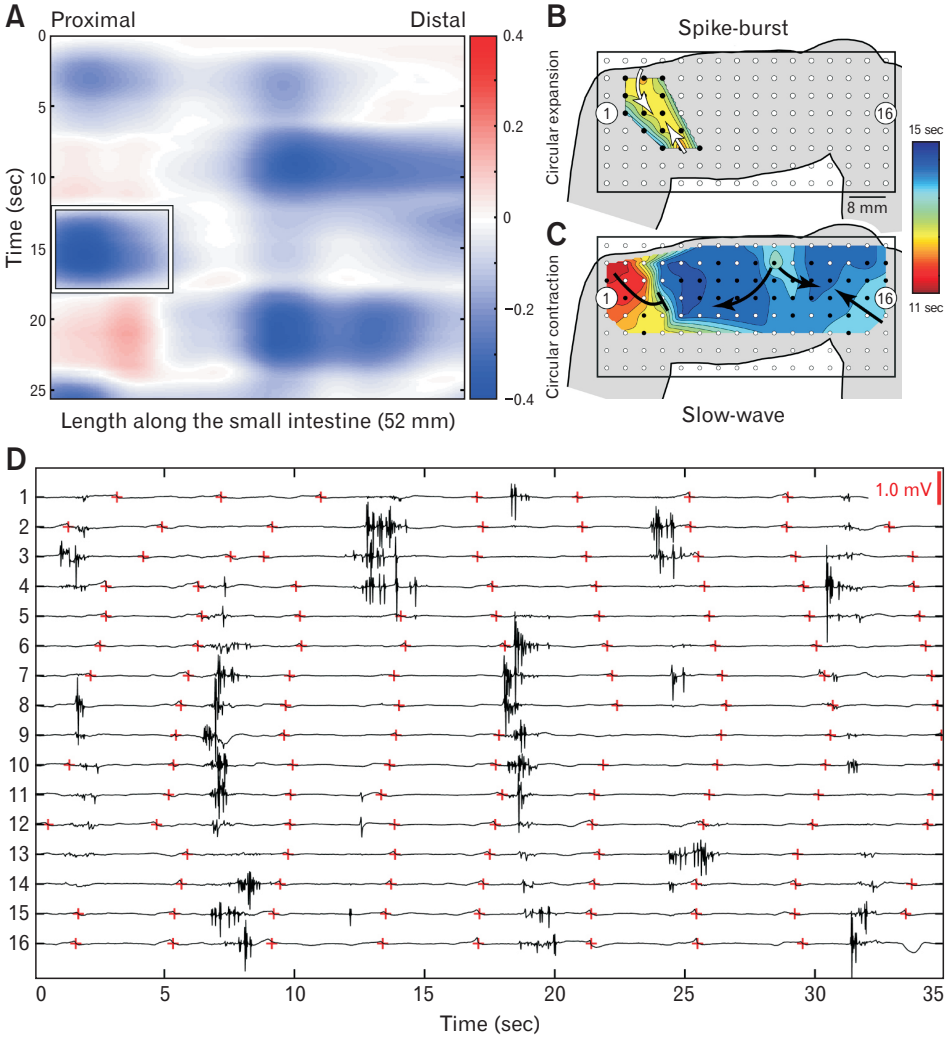

Figure 4. Slow-wave and spike-burst activity recorded during segmental contractions. (A) Spatiotemporal transverse strain map shows the segmental contractions and relaxations observed in the intestine. (B, C) Activation maps of the spike-burst and slow-wave activity just prior to the segmental contraction is marked by the white square in (A). The shaded area represents the position of the intestine on the electrode array. (D) The electrical signal traces from a row of electrodes with slow-wave events marked as red crosses. The region activated by the circumferential spike-burst patch in B underwent contraction as shown by the white square in (A). These spike-bursts and the corresponding contractions did not show a connection to the underlying slow-waves as seen in D. The spatiotemporal activation of slow-waves and spike-bursts during segmental contraction is shown in video form in Supplementary Video 1.

of the intestine then propagated along the length of the intestine as a sheath. The apparent propagation may also have been caused by the coordinated activation of multiple circumferential spike-burst patches one after the other. The spike-bursts were not coupled to the slow-waves as seen in the slow-wave activation map in Figure 5C and the electrical traces in Figure 5D. As a result, these peristaltic contractions spontaneously originated unrelated to the slow-wave propagation and propagated much slower than the underlying slow-wave velocity (3.7 ± 0.5 mm/sec contraction velocity vs 10.1 ± 4.7 mm/sec slow-wave velocity, $P = 0.007$). For instance, the spontaneous peristaltic contraction shown in Figure 5D (white arrow) spanned over 2 slow-wave cycles.

The spatiotemporal correlation of propagating circumferential spike-burst patches with spontaneous peristaltic contractions and their lack of correlation to slow-waves are more clearly shown in Supplementary Video 2.

Cyclic Peristaltic Contractions

Cyclic peristaltic contractions were observed in one rabbit study, and continuously occurred throughout the total recording duration of 17 minutes. These contractions were driven by slow-wave associated spike-bursts with a mean amplitude of 0.2 ± 0.1 mV and a mean duration of 0.2 ± 0.1 seconds. The underlying bioelectrical activity during cyclic peristalsis is shown in Figure 6. These longitudinally propagating circumferential contractions occurred periodically at a similar frequency to the underlying slow-waves (11.0 ± 0.6 cpm contraction frequency vs 10.8 ± 0.6 cpm slow-wave frequency, $P = 0.970$), and registered as periodic diagonal bands of negative strain in the transverse strain map (Fig. 6A). During these regularly propagating circumferential contractions, spike-bursts activated as longitudinally propagating circumferential spike-burst patches (Fig. 6B). The spike-bursts activated periodically with slow-wave cycles,

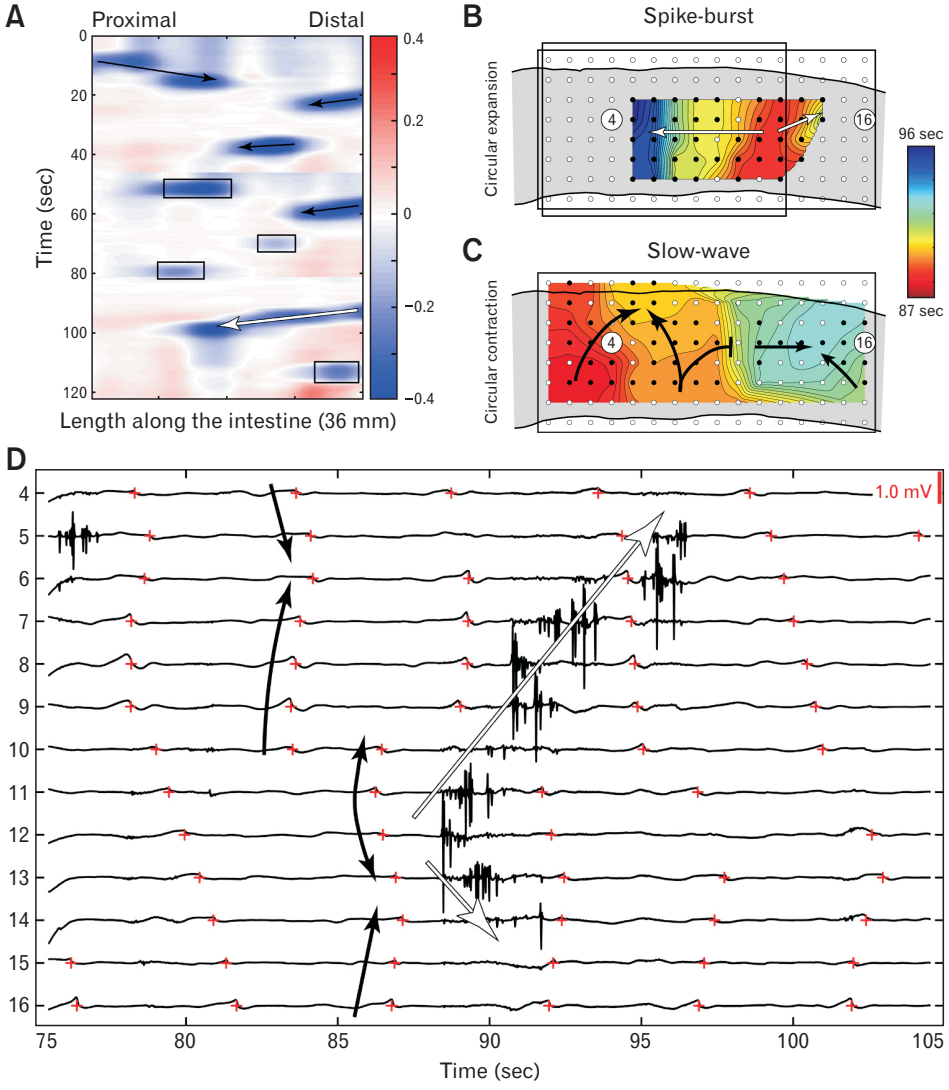

Figure 5. Slow-wave and spike-burst activity during spontaneous peristaltic contractions. (A) Spatiotemporal transverse strain map recorded during spontaneous peristaltic contractions. The spontaneous activation and propagation of these peristaltic contractions are indicated with arrows. Segmental contractions are indicated with rectangles. (B, C) Activation maps of spike-burst and slow-wave activity during the peristaltic contraction indicated by the white arrow in (A). The shaded area represents the position of the intestine on the electrode array. The black rectangle in (B) indicates the field of view of the camera. (D) Electrical signal traces from a row of electrodes with slow-wave events marked as red crosses. The white arrows indicate the propagating spike-bursts shown in (B) and the black arrows indicate the slow-wave propagation shown in (C). The spontaneous peristaltic contraction was caused by longitudinally propagating circumferential spike-burst patches as indicated by the white arrows. These peristaltic contractions and the spike-bursts did not show any connection to the slow-wave activity as seen in (D). The spatiotemporal activation of slow-waves and spike-bursts during spontaneous peristalsis is shown in video form in Supplementary Video 2.

which resulted in the continuous cyclic peristaltic contractions, as shown in the signal traces in Figure 6D. However, the propagation patterns of slow-waves and the spike-bursts deviated at times (Fig. 6B vs Fig. 6C). At the instance shown in Figure 6, slow-waves and the spike-bursts both originated at similar positions in the electrode array and propagated in either direction. The distal propagation of slow-waves was blocked by a conduction block at the center of the array, which did not affect the spike-bursts. Cyclic peristalsis caused shallower circumferential contractions compared to spontaneous peristalsis (17 ± 2% cyclic peristaltic contraction vs 36 ± 4% spontaneous peristaltic contraction, $P < 0.001$). In addition, cyclic peristaltic contractions propagated much faster than spontaneous peristalsis (14.2 ± 2.3 mm/sec cyclic peristalsis velocity vs 3.7 ± 0.5 mm/sec spontaneous peristalsis velocity, $P < 0.001$), which was closer to the underlying slow-wave propagation velocity (14.2 ± 2.3 mm/sec contraction velocity vs 11.5 ± 4.6 mm/sec slow-wave velocity, $P = 0.162$).

The spatiotemporal correlation of regularly propagating circumferential spike-burst patches with cyclic peristaltic contractions and their connection to slow-waves are more clearly shown in Supplementary Video 3.

Pendular Contractions

Pendular contractions were observed throughout the recording duration in 2 pigs and 2 rabbits as shown in Table. Pendular contractions were driven by slow-wave associated spike-bursts with mean amplitudes of 0.13 ± 0.06 mV in pigs, 0.09 ± 0.05 mV in rabbits, and mean durations of 0.8 ± 0.3 seconds in pigs, 0.5 ±

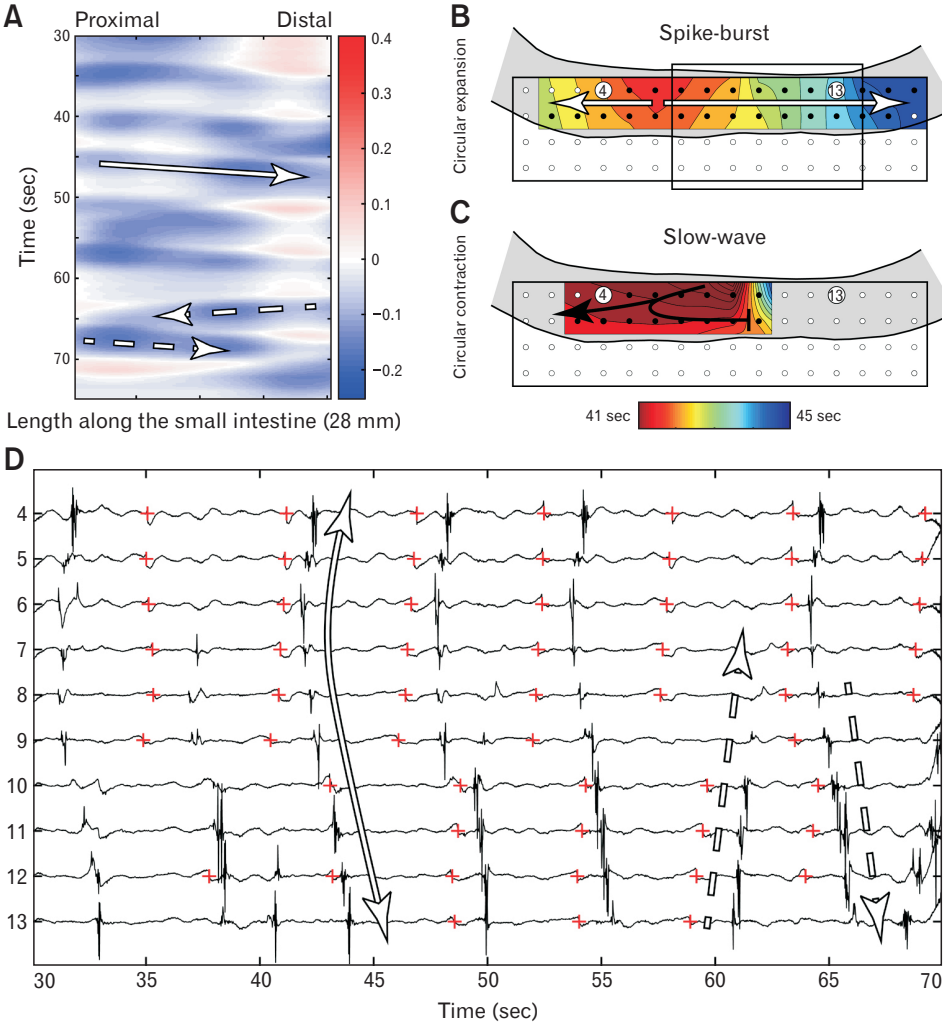

Figure 6. Slow-wave and spike-burst activity during cyclic peristalsis. (A) Spatiotemporal transverse strain maps which shows the regularly occurring propagating contractions of cyclic peristalsis. (B, C) Activation maps of spike-burst and slow-wave activity during the peristaltic contraction indicated by the solid arrow in (A). The shaded area represents the position of the intestine on the electrode array. The black rectangle in (B) indicate the field of view of the camera. (D) Electrical signal traces from a row of electrodes in (B, C), where red crosses indicate slow-wave events. The solid arrow indicates the spike-burst propagation shown in (B). The dash arrows show propagating spike-bursts from 2 slow-wave pacemakers that gave rise to the back-and-forth propagating contraction indicated with the dashed arrows in (A). Cyclic peristaltic contractions were caused by longitudinally propagating spike-burst patches that were associated with slow-waves as seen in (D). The spike-bursts activated periodically with the slow-waves causing propagating circumferential contractions at the frequency of the slow-waves. The spatiotemporal activation of slow-waves and spike-bursts during cyclic peristalsis is shown in video form in Supplementary Video 3.

0.2 seconds in rabbits. The underlying bioelectrical activity during pendular contractions is shown in Figure 7. Pendular contractions caused the intestine to longitudinally contract by 19 ± 6% in pigs, 12 ± 4% in rabbits, and registered as horizontal bands in the longitudinal strain map (Fig. 7A). During these longitudinal contractions, spike-bursts activated as longitudinal patches (Fig. 7B). The spike-bursts periodically activated with the slow-wave cycles as seen in the activation maps in Figure 7B and 7C and the electrical traces in Figure 7D. However, the propagation patterns of slow-waves and spike-bursts deviated at times. In the instance indicated by the dashed arrows in Figure 7D, a spike-burst from a distal slow-wave propagated beyond the slow-wave collision, deviating from the slow-wave activity. Furthermore, the spike-burst activity in the mesenteric and anti-mesenteric sides were not uniform, therefore, the contractions were also not uniform across the diameter. In the given instance, mesenteric side of the intestine displayed more activity than the anti-mesenteric side.

Discussion

This study simultaneously mapped slow-waves, spike-bursts, and motility in HR in the in vivo intestine. HR recordings showed that spike-burst patches correlate with the spatial domain that contracts. Motility patterns were primarily dictated by the pattern of the spike-burst patches (longitudinal or circumferential patches, non-propagating or propagating). The spike-bursts were sometimes coupled to the slow-waves and led to periodic motility patterns, but other times occurred independently to slow-waves and caused spontaneous aperiodic motility patterns.

Previous studies have shown that spike-bursts increase intraluminal pressure and outflow.[16,20] Here, we showed the spatiotemporal correlation between spike-burst patches and the sites of

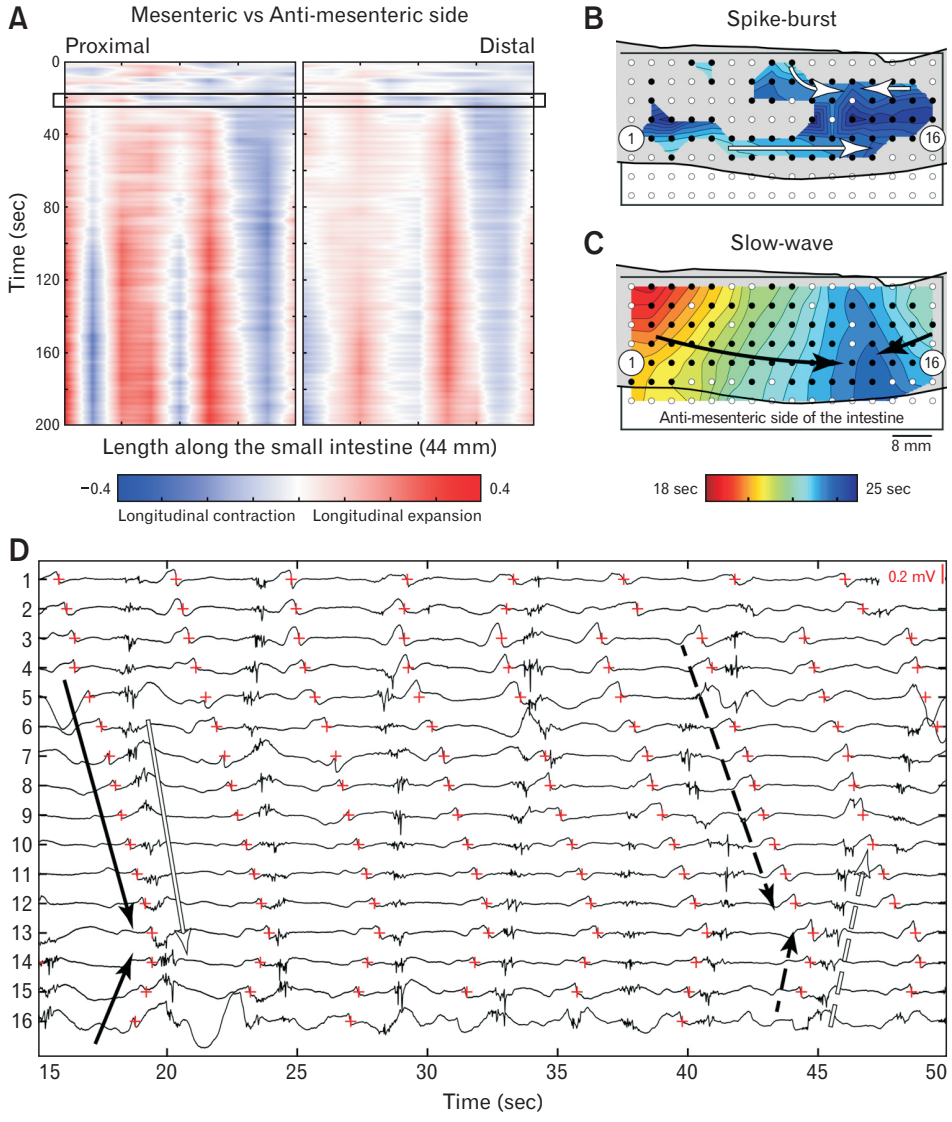

Figure 7. Slow-wave and spike-burst activity during pendular contractions. (A) Spatiotemporal longitudinal strain maps that show the longitudinal muscle activity in the mesenteric and anti-mesenteric side of the intestine. (B, C) Activation maps that show the propagation of slow-waves and spike-bursts during the time interval indicated by the rectangle in (A). The shaded area represents the position of the intestine on the electrode array. Spike-bursts activated as longitudinal patches. The spike-burst activity was different in the mesenteric and anti-mesenteric sides, and the contractile activity was also different as seen in (A). (D) Electrical signal traces from a row of electrodes with the slow-wave events marked as red crosses. The solid white arrow indicates the longitudinally propagating spike-burst shown in (B), and the solid black arrows indicate the propagating slow-wave shown in (C). The spike-bursts were associated with slow-waves, but the propagation patterns deviated at times. The dashed arrows indicate an instance where the spike-bursts of a distal slow-wave propagated beyond a slow-wave collision seemingly deviating from the slow-wave activity. The spatiotemporal activation of slow-waves and spike-bursts during pendular contractions is shown in video form in Supplementary Video 4.

contractions. Longitudinal spike-burst patches are likely calcium currents that trigger contractions in the longitudinal muscle layer, while circumferential spike-burst patches are likely calcium currents in the circular muscle layer.[28] As a result, these patches caused contractions in the respective directions. The amplitude, size, and energy of the spike-burst patches correlated with the level of deformation. Stronger correlations have been found between spike-burst patch amplitude, duration, size, and the rate of contraction.[37] These parameters are likely indications of the extent of the inward calcium currents.[17] A stronger calcium current may likely lead to a faster increase in the intracellular calcium concentration and therefore, led to a higher rate of contraction. It may also lead to a higher overall intracellular calcium concentration and therefore, caused a larger contraction.[7] A larger spike-burst patch size may result in the activation of a large portion of the muscle layer, therefore, caused a larger area of the tissue to undergo contraction. However, it should be noted that the calcium sensitivity of the smooth muscle cells can be changed by the presence of various enzymes, resulting in a varied contractile response for similar calcium concentrations.[38,39] This may have contributed to the high variance of the correlations.

Our data demonstrate that spike-burst propagation patterns ultimately dictated the resultant contractile response. Spike-burst patches occurred coupled to slow-wave activation at times, but also operated independent of slow-wave activation at other times, demonstrating that in the jejunum, slow-waves were not always correlated to the contractile response. Non-propagating circumferential spike-burst patches led to segmental contractions, while propagating circumferential spike-burst patches led to peristaltic

contractions. Propagating circumferential spike-burst patches that were independent of slow-waves led to spontaneous peristaltic contractions, and drew notable parallels to neurogenic peristalsis in the literature.[10,12,14,23] The descriptions of spontaneous peristalsis in guinea-pig colon,[14] peristalsis in cat intestine,[23] spontaneous emptying in guinea-pig intestine,[12] and peristalsis in W/W^{v} mouse intestine[10] are similar to the characteristics of spontaneous peristaltic contractions observed in this study. On the other hand, circumferential spike-burst patches associated with slow-waves led to cyclic peristaltic contractions, which displayed similar characteristics to partly or fully myogenic peristalsis in the literature.[10,14,15] Periodicity, propagation velocity in relation to slow-waves, level of deformation caused, and the underlying bioelectrical activity of cyclic peristaltic contractions were similar to propagating oscillations in mouse intestine,[15] myogenic ripples in guinea-pig colon,[14] and peristalsis in mouse intestine.[10]

Longitudinal spike-burst patches that were associated with slow-waves led to pendular contractions, confirming previous observations from 1-dimensional electrode arrays.[24] The results from HR electrode arrays validates the findings that predominant spatial activation of spike-bursts was in the longitudinal direction. In addition, we also identified that dissimilar contractions in the antimesenteric and mesenteric borders commonly observed during pendular contractions were due to different spike-burst activities in the respective borders.[40] Furthermore, the slow-wave associated spike-bursts indicate that myogenic mechanisms may be involved with pendular contractions. A previous study has reported that pendular contractions were not affected by the neural inhibitory agent tetrodotoxin, suggesting they are myogenically driven.[40] However, it should be noted that since the spike-bursts and concomitant pendular contractions were not uniform across the intestinal diameter, contractions quantified from the top surface of the intestine could not be accurately spatially correlated with the electrical events recorded from the bottom surface.

The slow-wave associated spike-bursts and independent spike-bursts observed here displayed similar characteristics to myogenic vs neurogenic spike-bursts observed in the colon,[22] and slow-wave associated spike-bursts vs peristaltic waves defined in the cat small intestine. Slow-wave associated spike-bursts had relatively lower amplitude and shorter duration similar to myogenic spike-bursts and slow-wave associated spike-bursts in cats. Independent spike-bursts had relatively higher amplitude and longer duration, similar to neurogenic spike-bursts and peristaltic waves. The affinity to slow-waves suggests that slow-wave associated spike-bursts are at least partly myogenically mediated. They occurred periodically with slow-waves and led to cyclic motility patterns modulated by slow-waves. The independent spike-bursts occurred irregularly and much less frequently than slow-wave associated spike-bursts. Independent spike-bursts could likely be activated by the firing of enteric neurons[41] and are unrelated to the underlying slow-waves. This would lead to motility patterns that are not driven by slow-waves. The higher amplitude and duration of independent spike-bursts suggest that they may be attributed to larger calcium currents than slow-wave associated spike-bursts. Slow-wave dependent calcium currents occur through voltage-dependent calcium channels.[7,42] Neurogenic mechanisms can cause calcium entry through multiple pathways.[42] For instance, the neurotransmitter acetylcholine can activate both transient receptor potential cation channels and intracellular calcium release.[42,43] The resulting rapid depolarization could also activate voltage-dependent calcium channels, which could lead to a larger inward calcium current compared to only voltage-dependent calcium channels in slow-wave associated spike-bursts, and accords with our results where independent spike-bursts correlated with larger deformations.

Although slow-wave associated spike-bursts occurred with the slow-wave cycles, their propagation patterns were not always identical to the slow-waves. Our results in this study suggest that spike-bursts can propagate along the intestine through 2 pathways: (1) the propagating slow-wave can initiate spike-bursts in smooth muscle cells in its path[7] where they would appear to propagate coupled to the slow-waves in the electrical recordings and (2) the initiated spike-bursts can also independently propagate along the smooth muscle layers[18] where the propagation would be predominantly in circumferential or longitudinal direction in the respective muscle layers.[28] The 2 modes of propagation are further evident by the fact that there was more deviation along the rows of electrodes during longitudinal patches (Fig. 7D), and less deviation during circumferential patches (Fig. 6D). The resulting spike-burst propagation would be through a combination of both of these methods, and therefore, could deviate from the slow-waves.

Furthermore, our observations indicate there may be an inhibitory relationship between independent spike-bursts and slow-wave associated spike-bursts. In one pig experiment, slow-wave associated spike-bursts were observed during baseline but were replaced by independent spike-bursts after distension. The mechanism behind the replacement of slow-wave associated spike-bursts with independent spike-bursts is not clear. A previous report in the colon has identified that neurogenic spike-burst activations inhibit myogenic spike-bursts and suggests that there may be some enteric neural control over the mechanisms underlying myogenic spike-bursts.[22]

Our observations indicate that a similar relationship between independent spike-bursts and slow-wave associated spike-bursts in the intestine could exist, however, would require further experimentation to inhibit certain pathways and verify these findings.

It should also be noted that there was a difference between the observed motility patterns in pigs and rabbits. Pigs displayed both slow-wave associated and independent spike-bursts along with corresponding contractions. In the rabbit studies, only slow-wave associated spike-bursts were observed along with corresponding contractions. As a result, spontaneous peristaltic contractions were observed only in pigs, while cyclic peristaltic contractions were observed only in the rabbit. However, it is possible that cyclic peristaltic contractions could occur in pigs, and slow-wave independent motility patterns could occur in rabbits,[42] although they were not observed in our experiments. It is plausible that differences in animal care procedures could have contributed to the observed discrepancy in the bioelectrical activity between pigs and rabbits. Pigs were fasted prior to the experiments, however, rabbits were not fasted prior to surgery, as this can lead to hypomotility and compromise gut function.[44] Studies have shown that slow-wave associated spike-bursts increase in the postprandial period, although the key pathways regulating this difference are yet to be elucidated.[45] There are also physiological differences between pigs and rabbits. The transit time of content through the rabbit small intestine is faster compared to other animals,[46] and therefore, cyclic peristalsis may be more prominent in rabbits than other species. In rabbits, small intestine motility is regulated in part by motilin, similar to humans and is in contrast to most other animal species.[46] However, motilin does not play a prominent role in pigs.[47] Therefore, observed bioelectrical and contraction patterns could have been influenced by animal care procedures and physiological variance.

This study successfully captured the slow-waves, spike-bursts, and motility simultaneously in the in vivo intestine. Nonetheless there are several limitations in the current study. First, the anesthesia and laparotomy could influence the electrical and mechanical activities of the gut, and could cause reflex inhibition.[48] The experimental setup could be further improved with multiple cameras to calculate strain in 3 dimensions, and the strain measurement could be supplemented with HR manometry to calculate the true mechanical state of the muscle.[49,50] Techniques such as optical mapping with voltage sensitive dyes could be used to measure the bioelectrical activity from the same surface of the intestine as the contractions.[51] Neural and myogenic inhibitory agents could also be used to elucidate the underlying regulatory mechanisms of bioelectrical and contractile coupling. For example, future studies that utilize ion channel blockers such as nifedipine, thapsigargin could be designed to evaluate the exact ionic pathways involved with slow-wave associated spike-bursts and independent spike-bursts.[42,52] It should also be noted that since motility was not modulated in this study, cyclic peristaltic contractions were only observed in 1 rabbit study. In future investigations, prokinetic agents such as domperidone,[53] metoclopromide,[54] and prucalopride[55] can be used to elicit specific motility patterns, to verify the findings of this study on a larger dataset.

In summary, this study defines in vivo intestinal motility patterns with simultaneous mapping of slow-waves and spike-bursts in spatiotemporal detail. The defined electrophysiological relationships between motility, slow-waves and spikes would aid in understanding the role of abnormal activity in functional motility disorders and would also be useful in computational physiological modeling.

Supplementary Materials

Note: To access the supplementary videos mentioned in this article, visit the online version of *Journal of Neurogastroenterology and Motility* at http://www.jnmjournal.org/, and at https://doi.org/10.5056/jnm21183.

Acknowledgements: The authors thank Linley Nisbet for her expert technical assistance.

Financial support: This work was supported by the Health Research Council of New Zealand (17/561), the Medical Technologies Center of Research Excellence (MedTech CoRE), and Riddet Institute Center of Research Excellence. Timothy R Angeli-Gordon was supported by a Rutherford Discovery Fellowship from the Royal Society Te Apārangi (RDF-18-UOA-023).

Conflicts of interest: No commercial support was received for any material presented in this publication. Leo K Cheng, Timothy R Angeli-Gordon, and Nira Paskaranandavadivel hold intellectual property and/or patent applications on gastrointestinal electrophysiology. Leo K Cheng, Timothy R Angeli-Gordon, and Nira Paskaranandavadivel are shareholders in FlexiMap Ltd.

Author contributions: Sachira Kuruppu, Leo K Cheng, and Nira Paskaranandavadivel designed the research study; and Sachira Kuruppu, Leo K Cheng, Recep Avci, Timothy R Angeli-Gordon, and Nira Paskaranandavadivel were involved in data collection, discussed the results, and contributed to the final manuscript.

References

1. Cheng LK, O'Grady G, Du P, Egbuji JU, Windsor JA, Pullan AJ. Gastrointestinal system. Wiley Interdiscip Rev Syst Biol Med 2010;2:65-79.
2. Huizinga JD, Lammers WJEP. Gut peristalsis is governed by a multitude of cooperating mechanisms. Am J Physiol Gastrointest Liver Physiol 2009;296:G1-G8.
3. Sanders KM, Koh SD, Ro S, Ward SM. Regulation of gastrointestinal motility-insights from smooth muscle biology. Nat Rev Gastroenterol Hepatol 2012;9:633-645.
4. Thomas PA, Akwari OE, Kelly KA. Hormonal control of gastrointestinal motility. World J Surg 1979;3:545-552.
5. Sanders KM. Regulation of smooth muscle excitation and contraction. Neurogastroenterol Motil 2008;20(suppl 1):39-53.
6. Thomsen L, Robinson TL, Lee JCF, et al. Interstitial cells of Cajal generate a rhythmic pacemaker current. Nat Med 1998;4:848-851.
7. Ozaki H, Stevens RJ, Blondfield DP, Publicover NG, Sanders KM. Simultaneous measurement of membrane potential, cytosolic Ca^{2+}, and tension in intact smooth muscles. Am J Physiol 1991;260(5 Pt 1):C917-C925.
8. Huizinga JD, Chen JH, Zhu YF, et al. The origin of segmentation motor activity in the intestine. Nat Commun 2014;5:3326.
9. Cannon WB. The movements of the intestines studied by means of the Röntgen rays. J Med Res 1902;7:72-75.
10. Huizinga JD, Ambrous K, Der-Silaphet T. Co-operation between neural and myogenic mechanisms in the control of distension-induced peristalsis in the mouse small intestine. J Physiol 1998;506:843-856.
11. Bogeski G, Shafton AD, Kitchener PD, Ferens DM, Furness JB. A quantitative approach to recording peristaltic activity from segments of rat small intestine in vivo. Neurogastroenterol Motil 2005;17:262-272.
12. Hennig GW, Costa M, Chen BN, Brookes SJH. Quantitative analysis of peristalsis in the guinea-pig small intestine using spatio-temporal maps. J Physiol 1999;517:575-590.
13. Melville J, Macagno E, Christensen J. Longitudinal contractions in the duodenum: their fluid mechanical function. Am J Physiol 1975;228:1887-1892.
14. D'Antona G, Hennig GW, Costa M, Humphreys CM, Brookes SJ. Analysis of motor patterns in the isolated guinea-pig large intestine by spatio-temporal maps. Neurogastroenterol Motil 2001;13:483-492.
15. Seerden TC, Lammers WJEP, De Winter BY, De Man JG, Pelckmans PA. Spatiotemporal electrical and motility mapping of distension-induced propagating oscillations in the murine small intestine. Am J Physiol Liver Physiol 2005;289:G1043-G1051.
16. Summers RW, Dusdieker NS. Patterns of spike burst spread and flow in the canine small intestine. Gastroenterology 1981;81:742-750.
17. Lammers WJ, Slack JR. Of slow waves and spike patches. News Physiol Sci 2001;16:138-144.
18. Stevens RJ, Publicover NG, Smith TK. Propagation and neural regulation of calcium waves in longitudinal and circular muscle layers of guinea pig small intestine. Gastroenterology 2000;118:892-904.
19. Noack T, Deitmer P, Lammel E. Characterization of membrane currents in single smooth muscle cells from the guinea-pig gastric antrum. J Physiol 1992;451:387-417.
20. Øigaard A, Dorph S. The relative significance of electrical spike potentials and intraluminal pressure waves as quantitative indicators of motility. Am J Dig Dis 1974;19:797-803.
21. Summers RW, Dusdieker NS. Patterns of spike burst spread and flow in the canine small intestine. Gastroenterology 1981;81:742-750.
22. Hibberd TJ, Costa M, Travis L, et al. Neurogenic and myogenic patterns of electrical activity in isolated intact mouse colon. Neurogastroenterol Motil 2017;29:1-12.
23. Lammers WJEP, Stephen B, Slack JR. Similarities and differences in the propagation of slow waves and peristaltic waves. Am J Physiol Liver Physiol 2002;283:G778-G786.
24. Lammers WJEP. Spatial and temporal coupling between slow waves and pendular contractions. Am J Physiol Liver Physiol 2005;289:G898-G903.
25. Du P, O'Grady G, Egbuji JU, et al. High-resolution mapping of in vivo gastrointestinal slow wave activity using flexible printed circuit board electrodes: methodology and validation. Ann Biomed Eng 2009;37:839-846.
26. Lammers WJEP, Stephen B, Arafat K, Manefield GW. High resolution electrical mapping in the gastrointestinal system: initial results. Neurogastroenterol Motil 1996;8:207-216.
27. Angeli TR, O'Grady G, Paskaranandavadivel N, et al. Experimental and automated analysis techniques for high-resolution electrical mapping of small intestine slow wave activity. J Neurogastroenterol Motil 2013;19:179-191.
28. Lammers WJEP, Donck L Ver, Schuurkes JAJ, Stephen B. Longitudinal and circumferential spike patches in the canine small intestine in vivo. Am J Physiol Liver Physiol 2003;285:G1014-G1027.
29. Kuruppu S, Cheng LK, Angeli TR, Avci R, Paskaranandavadivel N. A framework for spatiotemporal analysis of gastrointestinal spike burst propagation. Annu Int Conf IEEE Eng Biol Soc 2019;2019:4619-4622.
30. Kuruppu S, Cheng LK, Nielsen PMF, et al. High-resolution spatiotemporal quantification of intestinal motility with free-form deformation. IEEE Trans Biomed Eng 2022;69:2077-2086.
31. Cherian Abraham A, Cheng LK, Angeli TR, Alighaleh S, Paskaranandavadivel N. Dynamic slow-wave interactions in the rabbit small intestine defined using high-resolution mapping. Neurogastroenterol Motil 2019;31:e13670.
32. Yassi R, O'Grady G, Paskaranandavadivel N, et al. The gastrointestinal electrical mapping suite (GEMS): software for analyzing and visualizing high-resolution (multi-electrode) recordings in spatiotemporal detail. BMC Gastroenterol 2012;12:60.
33. Erickson JC, O'Grady G, Du P, Egbuji JU, Pullan AJ, Cheng LK. Automated gastric slow wave cycle partitioning and visualization for high-resolution activation time maps. Ann Biomed Eng 2011;39:469-483.
34. Paskaranandavadivel N, O'Grady G, Du P, Pullan AJ, Cheng LK. An improved method for the estimation and visualization of velocity fields from gastric high-resolution electrical mapping. IEEE Trans Biomed Eng 2012;59:882-889.
35. Wagenaar DA, Potter SM. Real-time multi-channel stimulus artifact

suppression by local curve fitting. J Neurosci Methods 2002;120:113-120.
36. Erickson JC, Velasco-Castedo R, Obioha C, Cheng LK, Angeli TR, O'Grady G. Automated algorithm for GI spike burst detection and demonstration of efficacy in ischemic small intestine. Ann Biomed Eng 2013;41:2215-2228.
37. Kuruppu S, Cheng LK, Angeli TR, Avci R, Paskaranandavadivel N. High-resolution mapping of intestinal spike bursts and motility. Annu Int Conf IEEE Eng Med Biol Soc 2020;2020:1779-1782.
38. Bitar KN. Function of gastrointestinal smooth muscle: From signaling to contractile proteins. Am J Med 2003:115(suppl 3A):15S-23S.
39. Gong MC, Fuglsang A, Alessi D, et al. Arachidonic acid inhibits myosin light chain phosphatase and sensitizes smooth muscle to calcium. J Biol Chem 1992;267:21492-21498.
40. Lentle RG, De Loubens C, Hulls CM, Janssen PWM, Golding MD, Chambers JP. A comparison of the organization of longitudinal and circular contractions during pendular and segmental activity in the duodenum of the rat and guinea pig. Neurogastroenterol Motil 2012;24:686-695, e298.
41. Spencer NJ, Hibberd TJ, Travis L, et al. Identification of a rhythmic firing pattern in the enteric nervous system that generates rhythmic electrical activity in smooth muscle. J Neurosci 2018;38:5507-5522.
42. Grasa L, Rebollar E, Arruebo MP, Plaza MA, Murillo MD. The role of Ca^{2+} in the contractility of rabbit small intestine in vitro. J Physiol Pharmacol 2004;55:639-650.
43. Tsvilovskyy VV, Zholos AV, Aberle T, et al. Deletion of TRPC4 and TRPC6 in mice impairs smooth muscle contraction and intestinal motility in vivo. Gastroenterology 2009;137:1415-1424.
44. Yorston M. Gastrointestinal stasis in rabbits. New Zeal Vet Nurse J 2013:26-29. Available from URL: https://www.nzvna.org.nz/site/nzvna/files/Quizzes/Rabbit%20Stasis.pdf (accessed 8 Sep, 2022).
45. Qian LW, Peters LJ, Chen JD. Postprandial response of jejunal slow waves and mediation via cholinergic mechanism. Dig Dis Sci 1999;44:1506-1511.
46. Davies RR, Davies JA. Rabbit gastrointestinal physiology. Vet Clin North Am Exot Anim Pract 2003;6:139-153.
47. Bueno L, Fioramonti J, Rayner V, Ruckebusch Y. Effects of motilin, somatostatin, and pancreatic polypeptide on the migrating myoelectric complex in pig and dog. Gastroenterology 1982;82:1395-1402.
48. Kock NG. An experimental analysis of mechanisms engaged in reflex inhibition of intestinal motility. Acta Physiol Scand 1959;47:1-54.
49. Dinning PG, Wiklendt L, Maslen L, et al. Quantification of in vivo colonic motor patterns in healthy humans before and after a meal revealed by high-resolution fiber-optic manometry. Neurogastroenterol Motil 2014;26:1443-1457.
50. Costa M, Wiklendt L, Arkwright JW, et al. An experimental method to identify neurogenic and myogenic active mechanical states of intestinal motility. Front Syst Neurosci 2013;7:7.
51. Zhang H, Yu H, Walcott GP, et al. High-resolution optical mapping of gastric slow wave propagation. Neurogastroenterol Motil 2019;31:e13449.
52. Angeli TR, Du P, Paskaranandavadivel N, et al. The bioelectrical basis and validity of gastrointestinal extracellular slow wave recordings. J Physiol 2013;591:4567-4579.
53. Ahmad N, Keith-Ferris J, Gooden E, Abell TL. Making a case for domperidone in the treatment of gastrointestinal motility disorders. Curr Opin Pharmacol 2006;6:571-576.
54. Eisner M. Effect of metoclopramide on gastrointestinal motility in man. A manometric study. Am J Dig Dis 1971;16:409-419.
55. Qi H Bin, Luo JY, Liu X. Effect of enterokinetic prucalopride on intestinal motility in fast rats. World J Gastroenterol 2003;9:2065-2067.